Published in final edited form as:
J Bone Miner Res. 2013 April ; 28(4): 865–874. doi:10.1002/jbmr.1807.

Sclerostin Antibody Inhibits Skeletal Deterioration Due to Reduced Mechanical Loading

Jordan M Spatz[1,2,3], **Rachel Ellman**[1,2], **Alison M Cloutier**[2], **Leeann Louis**[2], **Miranda van Vliet**[2], **Larry J Suva**[4], **Denise Dwyer**[5], **Marina Stolina**[5], **Hua Zhu Ke**[5], and **Mary L Bouxsein**[2,3,6]

[1]Harvard–Massachusetts Institute of Technology (MIT) Division of Health Sciences and Technology (HST), Bioastronautics Program, Cambridge, MA, USA

[2]Center for Advanced Orthopaedic Studies, Beth Israel Deaconess Medical Center, Boston, MA, USA

[3]Endocrine Division, Massachusetts General Hospital, Boston, MA, USA

[4]Department of Orthopedic Surgery, Center for Orthopaedic Research, University of Arkansas Medical School, Little Rock, AR, USA

[5]Amgen, Inc., Thousand Oaks, CA, USA

[6]Department of Orthopaedic Surgery, Harvard Medical School, Cambridge, MA, USA

Abstract

Sclerostin, a product of the SOST gene produced mainly by osteocytes, is a potent negative regulator of bone formation that appears to be responsive to mechanical loading, with *SOST* expression increasing following mechanical unloading. We tested the ability of a murine sclerostin antibody (SclAbII) to prevent bone loss in adult mice subjected to hindlimb unloading (HLU) via tail suspension for 21 days. Mice (n = 11–17/group) were assigned to control (CON, normal weight bearing) or HLU and injected with either SclAbII (subcutaneously, 25 mg/kg) or vehicle (VEH) twice weekly. SclAbII completely inhibited the bone deterioration due to disuse, and induced bone formation such that bone properties in HLU-SclAbII were at or above values of CON-VEH mice. For example, hindlimb bone mineral density (BMD) decreased –9.2%±1.0% in HLU-VEH, whereas it increased 4.2%±0.7%, 13.1%±1.0%, and 30.6%±3.0% in CON-VEH, HLU-SclAbII, and CON-SclAbII, respectively ($p < 0.0001$). Trabecular bone volume, assessed by micro–computed tomography (μCT) imaging of the distal femur, was lower in HLU-VEH versus CON-VEH ($p < 0.05$), and was 2- to 3-fold higher in SclAbII groups versus VEH ($p < 0.001$). Midshaft femoral strength, assessed by three-point bending, and distal femoral strength, assessed by micro–finite element analysis (μFEA), were significantly higher in SclAbII versus VEH-groups in both loading conditions. Serum sclerostin was higher in HLU-VEH (134±5 pg/mL) compared

Address correspondence to: Mary L Bouxsein, Center for Advanced Orthopedic Studies, Beth Israel Deaconess Medical Center, 330 Brookline Ave, Boston, MA 02215. mbouxsei@bidmc.harvard.edu.

Disclosures

DD, MS, and HZK are employed by Amgen, Inc., and own Amgen stock. All other authors state that they have no conflicts of interest.

to CON-VEH (116±6 pg/mL, $p < 0.05$). Serum osteocalcin was decreased by hindlimb suspension and increased by SclAbII treatment. Interestingly, the anabolic effects of sclerostin inhibition on some bone outcomes appeared to be enhanced by normal mechanical loading. Altogether, these results confirm the ability of SclAbII to abrogate disuse-induced bone loss and demonstrate that sclerostin antibody treatment increases bone mass by increasing bone formation in both normally loaded and underloaded environments.

Keywords

BONE LOSS; HINDLIMB UNLOADING; SCLEROSTIN ANTIBODY; BONE; MOUSE; BONE DENSITY

Introduction

Mechanical loading is required for the development and maintenance of skeletal integrity, whereas weightlessness and immobility, as experienced by bedridden, immobilized patients or astronauts, leads to reduced bone mass and strength.[1] Although the exact nature of mechanosensing in bone is incompletely understood, osteocytes appear to be a prominent cellular orchestrator of mechanotransduction in bone.[2–5] The osteocyte secreted protein sclerostin, a product of the SOST gene, is a major negative regulator of bone formation and appears to be responsive to mechanical loading, as its expression increases with mechanical unloading and decreases with loading.[6,7] Further, SOST knockout mice are resistant to bone loss in the hindlimb unloading model.[8]

Pharmacologic inhibition of sclerostin induces bone formation in normal and ovariectomized animals that are fully weight-bearing[9–13] and also following unilateral limb immobilization in rats.[14] Also, there is only a short-term (7 days) study that has examined sclerostin antibody treatment in the well-characterized hindlimb unloading (HLU) model.[15] However, because of the limited duration of unloading, this study did not demonstrate bone microarchitectural changes due to HLU, nor report effects on bone mechanical properties of unloading or sclerostin antibody treatment. Further, there are conflicting reports in the literature as to whether the optimal anabolic effect of sclerostin antibody treatment requires normal mechanical loading.[9,14,15] Finally, although there is evidence that *SOST* is increased by mechanical unloading,[6,16] there is limited data on serum levels of sclerostin following reduced mechanical loading in animal models.

Thus, in this study we sought to demonstrate the anabolic effects of pharmacologic inhibition of sclerostin in the HLU model. We hypothesized that sclerostin antibody treatment would not only inhibit bone loss and the deterioration of mechanical properties associated with disuse-induced bone loss, but would also induce bone formation. We also determined whether the skeletal effects of sclerostin antibody treatment depend on mechanical loading by comparing the response to pharmacologic inhibition in normally loaded animals to those exposed to HLU, and by comparing the responses in the forelimbs and hindlimbs of HLU mice. Finally, we determined whether serum sclerostin increased following HLU to elucidate whether in addition to SOST, the sclerostin protein is mechanically regulated by disuse.

Materials and Methods

Overview of study design

Female adult mice (C57Bl/6J, 12 weeks of age; Jackson Laboratory, Bar Harbor, ME, USA) were subjected to either HLU via tail suspension,[17] or normal loading (CON) and injected twice weekly with sclerostin antibody (SclAbII, 25 mg/kg, subcutaneously; Amgen, Thousand Oaks, CA, USA) or vehicle (VEH) for the 21-day experiment. Thus, mice were assigned to one of four groups: HLU-VEH (n = 13), HLU-SclAbII (n = 11), CON-VEH (n = 17), or CON-SclAbII (n = 11). Animals were assigned to groups by total body bone mineral density (BMD) and body mass in a manner to minimize differences between groups at baseline. All mice were weighed daily for the first 5 days and biweekly thereafter, with adjustments made to ensure the hindlimb paws could not touch the ground. The average weight-bearing on the forelimbs of HLU groups was 43% 1.4% of total body mass. Mice were maintained on a 12/12 hour light/dark cycle and had *ad libitum* access to standard laboratory rodent chow and water. Control animals were singly housed to mimic the increased stress environment of singly housed HLU animals. Mice were euthanized by CO_2 inhalation at the end of the experiment. All animal procedures were approved by and performed in accordance with the guidelines of the Institutional Animal Care and Use Committee (IACUC) at the Beth Israel Deaconess Medical Center.

Bone mineral density and body composition

In vivo assessment of total body (exclusive of the head region), hindlimb, and forelimb BMD (g/cm^2) was performed at baseline and end of the study using peripheral dual-energy X-ray absorptiometry (pDXA PIXImusII; GE Lunar Corp., Madison, WI, USA), as described.[18]

Specimen harvesting and preparation

Femurs, tibias, and humeri were harvested and cleaned of soft tissue. The right femurs and humeri and were prepared for imaging and biomechanical testing by wrapping in saline-soaked gauze and freezing at –20°C. The left femur was prepared for histology in 10% neutral buffered formalin at 4°C for 48 to 72 hours, and then transferred to 70% ethanol at 4°C. Wet weight of the gastrocnemius and soleus muscles were obtained at the end of the study, and normalized to body weight.

Bone turnover markers

Mice were fasted for 2 hours before blood was collected at the time of euthanasia. Serum was used to measure sclerostin (in VEH-treated mice only) and bone turnover markers. Osteocalcin and sclerostin (in VEH-treated mice only) were assessed using the species-specific single-plex Luminex assays (Millipore, Billerica, MA, USA). Serum concentrations of amino-terminal propeptide of type I procollagen (P1NP), tartrate-resistant acid phosphatase 5b (TRACP5b), and type I collagen C-telopeptide (sCTX) were measured by using mouse ELISA kits (IDS, Fountain Hills, AZ, USA). All assays were run according to the manufacturers' protocols.

Histology and quantitative histomorphometry

Qualitative histologic analysis and quantitative static and dynamic histomorphometry were performed as described.[18] To examine bone formation rates, calcein (15 mg/kg) was injected intraperitoneally at 8 days and alizarin red or demeclocycline 2 days prior to euthanasia. Histomorphometric measurements were performed on the secondary spongiosa of the distal femoral metaphysis using an OsteoMeasure morphometry system (Osteometrics, Atlanta, GA, USA). For dynamic histomorphometry, mineralizing surface per bone surface (MS/BS, %) and mineral apposition rate (MAR, μm/d) were measured in unstained sections under ultraviolet light, and used to calculate bone formation rate with a surface referent (BFR, $\mu m^3/\mu m^2/d$). Eroded surface per bone surface (ES/BS, %), number of osteoblasts, osteoclasts per bone surface, number of osteocytes per bone area (identified as filled lacunae), and number of adipocytes per marrow area were also measured, as described.[18] Terminology and units follow the recommendations of the Histomorphometry Nomenclature Committee of the American Society for Bone and Mineral Research.[19]

Mechanical testing

Femurs were mechanically tested at a constant displacement rate of 0.03 mm/s to failure in three-point bending (Bose ElectroForce 3200 with 150 N load cell; Bose Corporation, Eden Prairie, MN, USA). Fresh-frozen femurs were thawed to room temperature then centered longitudinally, with the anterior surface on the two lower support points spaced 10 mm apart.[20] Force-displacement data were acquired at 30 Hz and used to determine maximum force (N) and stiffness (N/mm). Assessment of bone morphology and microarchitecture was performed with high-resolution micro–computed tomography (μCT40; Scanco Medical, Brüttisellen, Switzerland). In brief, the distal femoral and humeral metaphysis were scanned using 70 KvP, 50 mAs, and 12-μm isotropic voxel size. The femoral metaphysis region began 240 μm distal to the growth plate and extended 1.8 mm distally. Similarly, the humeri region began 240 μm distal to the growth plate and extended 1.2 mm distally. Cancellous bone was separated from cortical bone with a semiautomated contouring program. For the cancellous bone region we assessed bone volume fraction (BV/TV, %), trabecular thickness (Tb.Th, mm), trabecular separation (Tb.Sp, mm), trabecular number (Tb.N, 1/mm), connectivity density (ConnD, $1/mm^3$), and structure model index (SMI). Transverse CT slices were also acquired at the femoral midshaft to assess total cross-sectional area, cortical bone area, and medullary area (TA, BA, and MA, respectively, all mm^2); bone area fraction (Ct.BA/TA, %), cortical thickness (Ct.Th, mm), porosity (Ct.Po, %) and minimum (Imin, mm^4), maximum (Imax, mm^4), and polar (pMOI, mm^4) moments of inertia. Cortical bone was analyzed from the metaphysis (surrounding the trabecular volume of interest) and from a 0.6-mm-long mid-diaphyseal region. Bone was segmented from soft tissue using the same threshold, 247 mg HA/cm^3 for trabecular and 672 mg HA/cm^3 for cortical bone. Scanning and analyses adhered to recently published guidelines.[21]

To assess the effect of unloading and sclerostin antibody treatment on mechanical properties of metaphyseal bone, μCT-derived data was used to perform linear micro–finite element analysis (μFEA) of the distal femur using the manufacturer's software (Scanco Medical AG, Bassersdorf, Switzerland), which implements a voxel-based μFEA method.[22] The μFE model of the metaphyseal region, including both cortical and trabecular bone, was subjected

to applied uniaxial compression, with an elastic modulus of 10 GPa and Poisson's ratio of 0.3 for each element. Outcomes included axial stiffness (N/mm) as well as the percentage of load carried by the cortical and trabecular compartments.

Statistical analysis

All data were checked for normality, and standard descriptive statistics computed. Treatment effects were evaluated using analysis of variance (ANOVA) or repeated measures ANOVA for all continuous variables. We used two-factor ANOVA to determine whether the effect of sclerostin antibody treatment depended on the loading condition. Main ANOVA effects and post hoc testing were considered significant at $p < 0.05$, whereas the interaction between treatment and loading was considered significant at $p < 0.1$. Data are reported as mean ±SEM, unless noted.

Results

Body mass

Body mass increased slightly in the CON-VEH and CON-SclAbII groups and declined transiently in the HLU groups in the first 3 days by –8% to –9% but then stabilized at –5% below baseline for remainder of study ($p < 0.05$ versus baseline). As a result, the HLU-SclAbII and HLU-VEH weighed less than their respective CON groups at the end of the study (–9.1% and –11.5%, respectively, $p < 0.05$).

Muscle mass

Soleus wet weight was 51% and 38% lower than CON in HLU-SclAbII and HLU-VEH, respectively ($p < 0.0001$, Fig. 1*A*). Gastrocnemius wet weight was 27% and 19% lower than CON in HLU-SclAbII and HLU-VEH, respectively ($p < 0.0001$, Fig. 1*B*). There were no differences in muscle mass between VEH-treated and SclAbII-treated groups in either loading condition.

BMD

BMD increased slightly in CON-VEH at all sites, whereas HLU caused significant bone loss at the hindlimb and total body, but not the forelimb (Fig. 2). Treatment with sclerostin antibody not only prevented the bone loss due to HLU, but led to marked increases in BMD in CON and HLU groups, both versus baseline and versus VEH-treated groups. For example, hindlimb BMD declined –9.3%±1.1% in HLU-VEH, whereas it increased 4.3% ±0.7%, 13.2%±1.0%, and 30.6%±3.0% versus baseline in CON-VEH, HLU-SclAbII, and CON-SclAbII, respectively ($p < 0.001$ for all). The pattern was similar for total body BMD (Fig. 2*A*). Forelimb BMD was unchanged in HLU-VEH (–1.1%±2.6%) and tended to increase in CON-VEH (4.1%±3.0%, $p = 0.2$ versus baseline). Forelimb BMD increased in SclAbII-treated HLU (15.1%±2.9%, $p < 0.001$ versus baseline) and CON groups (28.6% ±2.4%, $p < 0.001$, Fig. 2*C*); and these increases were significantly greater than the BMD changes in VEH-treated animals ($p < 0.0001$ for both).

Bone microarchitecture

Consistent with hindlimb BMD measurements, HLU resulted in significant bone deterioration, particularly in the trabecular compartment (Fig. 3, Table 1). Compared to CON-VEH, HLU-VEH mice had lower Tb.BV/TV, Tb.N, and Tb.Th in the distal femur. Cortical bone was also negatively affected by unloading, because HLU-VEH had lower cortical bone area, cortical bone area fraction, cortical thickness, and polar moment inertia than fully loaded animals at both the distal femoral and mid-diaphyseal sites (Table 1). In addition, HLU-VEH had higher cortical porosity than CON-VEH at the distal femoral cortex. At the humerus, trabecular bone parameters were unaffected by HLU; however, cortical bone area, bone area fraction, thickness, and polar moment of inertia were slightly lower in HLU-VEH versus CON-VEH (Table 2).

Treatment with SclAbII improved bone properties in normally loaded animals and fully inhibited disuse-induced bone loss, improving cortical and trabecular bone parameters to levels at or above the fully-loaded VEH-treated group. Specifically, SclAbII-treated animals, both loaded and unloaded, had significantly higher Tb.BV/TV, Tb.Th, and Tb.N, along with lower Tb.Sp, better connectivity density, and more plate-like architecture (SMI) than VEH-treated animals at both the femur and humerus (Tables 1 and 2). Treatment with SclAbII also improved cortical bone properties in both loaded and unloaded animals, increasing cortical bone area, thickness, and bone area fraction at both the femur and humerus, and prevented the increase in cortical porosity seen in the HLU group. SclAbII treatment led to lower midshaft medullary area in both HLU and CON, consistent with endocortical bone apposition. Mid-femoral cross-sectional area was increased in CON-SclAbII, but not HLU-SclAbII, suggesting that normal loading may augment SclAbII treatment's ability to induce periosteal bone apposition. Consistent with this, SclAbII treatment led to increased mid-diaphyseal cross-sectional area in the humeri of both the loaded and unloaded animals (Table 2).

The positive effect of SclAbII treatment was significantly greater in loaded than unloaded animals for femur Tb.BV/ TV, Tb.Th, and SMI, and midshaft cortical bone area (Fig. 3, Table 1, $p_{interaction} < 0.001$), and for Tb.BV/TV and Tb.Th in the proximal humerus.

Mid-femoral biomechanics and μFEA of the distal femoral metaphysis

Femoral bending stiffness and maximum load were 19% lower in HLU-VEH compared to CON-VEH ($p < 0.05$, Fig. 4). Mice treated with SclAbII had better mechanical properties compared to VEH-treated groups in both loading conditions, with maximum load and bending stiffness 40% to 50% higher than VEH (Fig. 4).

μFEA showed that compressive stiffness of the combined cortical and trabecular regions was 18% lower in HLU-VEH than CON-VEH ($p < 0.05$) and 50% higher in SclAbII versus VEH-treated mice in both loading conditions (Fig. 5A). Interestingly these changes in stiffness were nearly twofold greater than the respective changes in bone volume (–10% for HLU-VEH and +25% for SclAbII-treated animals), suggesting that changes in bone mass underestimate changes in mechanical properties.

HLU did not change the distribution of load sharing between the trabecular and cortical compartments. In contrast, the proportion of load carried by trabecular and cortical bone compartments were increased and decreased, respectively, in SclAbII-treated mice compared to VEH groups, consistent with a shift toward more uniform load sharing following SclAbII treatment in both loading conditions (Fig. 5). Notably, differences in μFEA-estimated stiffness (–18% in HLU-VEH versus CON-VEH, and +50% in SclAbII-treated mice) were larger than the differences in total bone volume (–10% in HLU-VEH versus CON-VEH, and +25% in SclAbII-treated mice), suggesting that changes in bone mass alone underestimate the effects of unloading and sclerostin antibody treatment on bone biomechanical properties.

Serum sclerostin and bone turnover markers

HLU-VEH mice had higher serum sclerostin (134±5 versus 116±6 pg/mL, $p < 0.05$), lower osteocalcin, and lower CTX1 than CON-VEH, but similar TRACP5b (Fig. 6). Compared to VEH-treated mice, those treated with SclAbII had higher osteocalcin and lower TRACP5b (in HLU only), but had similar CTX1 levels (Fig. 6).

Histomorphometry

Static and dynamic histomorphometry results are summarized in Table 3. Due to technical issues with fluorescent label incorporation in some animals, sample sizes in some groups were limited to 3 animals for dynamic outcomes. In VEH-treated animals, HLU led to reduced MAR and greater marrow adiposity. SclAbII treatment led to significantly higher bone formation indices (MAR, MS/BS, and BFR/BS) compared to VEH-treated mice in both loading conditions, but had no effect on marrow adiposity.

Discussion

The primary objective of this study was to determine the musculoskeletal effects of pharmacologic inhibition of sclerostin in mice exposed to hindlimb unloading. We hypothesized that sclerostin antibody treatment would prevent bone loss and the deterioration of mechanical properties associated with disuse by promoting bone formation. Treatment with sclerostin antibody led to skeletal anabolic activity in the setting of unloading, as evidenced by increases in BMD, trabecular and cortical microarchitecture, and femoral strength values in the HLU-SclAbII group that were at or above values in the CON-VEH group. Furthermore, treatment with sclerostin antibody resulted in an increase in serum bone formation markers and histologic evidence of enhanced trabecular bone formation. These observations of skeletal anabolic activity following treatment with sclerostin antibody in disuse are consistent with other studies of sclerostin antibody treatment during immobilization in rodents.[7,8] Further, the increases in total body and hindlimb BMD observed in our normally loaded control animals induced by sclerostin antibody treatment were similar to prior observations in normally loaded animals.[11,14,23] In addition, serum bone turnover markers and dynamic histomorphometry outcomes were consistent with sclerostin antibody treatment increasing bone mass in rodents mainly by enhancing bone formation.[14,15]

Sclerostin antibody treatment had inconsistent effects on indices of bone resorption, with decreased serum TRACP5b levels, but no differences in serum CTX. Serum was collected only at a single time point (eg, end of study) and thus the serum measures cannot reflect the changes over the entire experiment in osteoclast number versus their net activity that are theoretically reflected in the TRACP5b and CTX measures, respectively. Other studies in rodents have also reported declines in TRACP5b following sclerostin antibody treatment.[15,24]

The current study also explored whether the skeletal effects of sclerostin antibody treatment are sensitive to mechanical loading by examining effects in hindlimb-unloaded versus fully-loaded controls, and effects in the unloaded hindlimb versus loaded forelimb. In the femur, the skeletal response to sclerostin inhibition tended to be enhanced in the normally loaded mice compared to those exposed to hindlimb suspension, with significantly greater response in trabecular bone volume and microarchitecture, cortical bone area and thickness, and distal femur μFEA-estimated stiffness, as well as a trend for greater gain in leg BMD ($p = 0.20$ for load-treatment interaction). Furthermore, femoral midshaft cross-sectional area was greater than VEH-treated mice only in the fully loaded SclAbII-treated animals, suggesting that periosteal apposition induced by sclerostin inhibition requires mechanical loading. At the humerus, whereas the effects of sclerostin antibody on BMD and cortical bone morphology were similar in HLU and fully-loaded groups, the increases in trabecular bone volume, number, and thickness were greater in CON than HLU. Although speculative, the finding that the response to sclerostin inhibition is altered in the “loaded” humerus of the HLU group suggests that systemic effects of HLU (ie, stress) that are unrelated to mechanical loading influence the response to sclerostin inhibition. In a study of rats exposed to unilateral hindlimb immobilization via bandages, Tian and colleagues[14] also found that the trabecular bone response to sclerostin inhibition tended to be enhanced in the loaded versus unloaded limbs, whereas responses in cortical bone were similar in both groups. In contrast, in rats injected unilaterally with botulinum toxin A (botox) to induce hindlimb paralysis, the response to sclerostin inhibition was similar in the loaded and unloaded proximal tibia primary spongiosa.[9]

Although far from conclusive, taken together these observations suggest that the anabolic effects of sclerostin inhibition are enhanced with normal mechanical loading. As proposed by Tian and colleagues,[14] the relative excess of sclerostin in unloaded bone could reduce the anabolic effects of sclerostin inhibition relative to those seen in fully loaded bone. Alternatively, although sclerostin appears to be a central mediator of the bone's response to mechanical loading,[6,25] it may not be the only mechanism by which the osteocytic network responds to mechanical unloading. For example, another mechanism by which osteocytes may orchestrate a response to altered mechanical loading is suggested by the observation that osteocytes are a major source of the osteoclastogenic cytokine receptor activator of NF-κB ligand (RANKL),[26] and further, that mice lacking RANKL in osteocytes are protected from bone loss induced by hindlimb unloading.[4] Thus, sclerostin-independent effects, notably RANKL-mediated effects or, for example, the detrimental effects of increased marrow adiposity on osteo-blasts, could also be responsible for a differential response to sclerostin antibody treatment in unloaded versus loaded bone. Clearly, further studies are

needed to further investigate the interaction between mechanical loading and the anabolic effects of sclerostin antibody treatment.

Hindlimb unloading caused an increase in marrow adiposity, as reported.[27] Interestingly, sclerostin antibody treatment did not prevent the increased marrow adiposity with HLU and had no effect on marrow adiposity in normally loaded animals. Canonical Wnt signaling inhibits adipogenesis and promotes survival of committed preadipocytes.[28,29] Patients with activating mutations in low-density lipoprotein receptor-related protein 5 (LRP5) leading to increased Wnt signaling are associated with increased trabecular bone volume and reduced bone marrow fat in iliac crest biopsies, as well as increased osteogenesis and reduced adipogenesis of mesenchymal stem cells.[30] However, specific Wnt targets and the role of noncanonical Wnt signaling in adipogenesis remain incompletely understood.[31] Because sclerostin binds to the LRP4/5/6 receptor to inhibit Wnt signaling, our observation that sclerostin antibody treatment had no influence on bone marrow adiposity suggests that other mechanisms besides sclerostin-mediated Wnt signaling must be involved in the increased marrow adiposity seen with unloading.

Several limitations of this study merit mention. We studied only female mice at one time point, with a single-dosing regimen for sclerostin inhibition. Thus it is not clear whether the anabolic effects of sclerostin antibody would continue with longer treatment, or whether a higher dose or more frequent dosing would promote even greater anabolic effects in the skeleton or eliminate the load-treatment interactions we observed.

These limitations notwithstanding, this study provides novel information about the ability of sclerostin antibody to induce bone formation in the situation of reduced mechanical loading. We showed that changes in bone volume underestimate both the loss of bone strength with disuse and the gain of bone strength with sclerostin inhibition, and we also explored the question whether the anabolic actions of sclerostin inhibition are influenced by mechanical loading by comparing the skeletal responses of HLU and CON mice at both the forelimbs and hindlimbs.

In summary, treatment with sclerostin antibody induces an anabolic skeletal response in an established rodent model of disuse-induced bone loss, such that unloaded animals treated with sclerostin antibody had BMD, microarchitecture, and mechanical strength values at or above the normally loaded control mice. These results provide strong rationale for testing the ability of sclerostin antibody treatment to improve skeletal fragility in patients with spinal cord injuries, stroke, muscular dystrophy, cerebral palsy, and other diseases and conditions associated with short-term or chronic disuse.

Acknowledgments

This work was funded by NIH R21 AR057522, NASA NNX10AE39G, the National Space Biomedical Research Institute through NASA NCC 9-58, and a research grant from Amgen. RE was supported by a NASA-Jenkins predoctoral fellowship. JMS was supported by a Northrop Grumman Aerospace Systems PhD Training Fellowship.

Authors' roles: JMS: study design and conduct; data collection, analysis, and interpretation; manuscript drafting, revision, and approval. RE: study design and conduct; data collection and analysis; manuscript revision and approval. AMC, LL, MVV: study conduct, data collection and analysis; manuscript approval. LJS: histomorphometric measurements and analysis; manuscript revision and approval. DD, MS: serum measurements

and analysis; manuscript revision and approval. HZK: study design, manuscript revision and approval. MLB: study design; data analysis and interpretation; manuscript drafting, revision, and approval. JMS and MLB take responsibility for the integrity of the data analysis.

References

1. Smith SM, Heer MA, Shackelford L, Sibonga JD, Ploutz-Snyder L, Zwart SR. Benefits for bone from resistance exercise and nutrition in long-duration spaceflight: evidence from biochemistry and densitometry. J Bone Miner Res. Sep; 2012 27(9):1896–906. [PubMed: 22549960]
2. Krempien B, Manegold C, Ritz E, Bommer J. The influence of immobilization on osteocyte morphology: osteocyte differential count and electron microscopical studies. Virchows Arch A Pathol Anat Histol. 1976; 370:55–68. [PubMed: 818789]
3. Rodionova NV, Oganov VS, Zolotova NV. Ultrastructural changes in osteocytes in microgravity conditions. Adv Space Res. 2002; 30:765–70. [PubMed: 12528727]
4. Xiong J, Onal M, Jilka RL, Weinstein RS, Manolagas SC, O'Brien CA. Matrix-embedded cells control osteoclast formation. Nat Med. 2011; 17:1235–41. [PubMed: 21909103]
5. Aguirre JI, Plotkin LI, Stewart SA, Weinstein RS, Parfitt AM, Manolagas SC, Bellido T. Osteocyte apoptosis is induced by weightlessness in mice and precedes osteoclast recruitment and bone loss. J Bone Miner Res. 2006; 21:605–15. [PubMed: 16598381]
6. Robling AG, Niziolek PJ, Baldridge LA, Condon KW, Allen MR, Alam I, Mantila SM, Gluhak-Heinrich J, Bellido TM, Harris SE, Turner CH. Mechanical stimulation of bone in vivo reduces osteocyte expression of Sost/sclerostin. J Biol Chem. 2008; 283:5866–75. [PubMed: 18089564]
7. Moustafa A, Sugiyama T, Prasad J, Zaman G, Gross TS, Lanyon LE, Price JS. Mechanical loading-related changes in osteocyte sclerostin expression in mice are more closely associated with the subsequent osteogenic response than the peak strains engendered. Osteoporos Int. 2012; 23:1225–34. [PubMed: 21573880]
8. Lin C, Jiang X, Dai Z, Guo X, Weng T, Wang J, Li Y, Feng G, Gao X, He L. Sclerostin mediates bone response to mechanical unloading through antagonizing Wnt/beta-catenin signaling. J Bone Miner Res. 2009; 24:1651–61. [PubMed: 19419300]
9. Agholme F, Isaksson H, Li X, Ke HZ, Aspenberg P. Anti-sclerostin antibody and mechanical loading appear to influence metaphyseal bone independently in rats. Acta Orthop. 2011; 82:628–32. [PubMed: 22103277]
10. Li X, Warmington KS, Niu QT, Asuncion FJ, Barrero M, Grisanti M, Dwyer D, Stouch B, Thway TM, Stolina M, Ominsky MS, Kostenuik PJ, Simonet WS, Paszty C, Ke HZ. Inhibition of sclerostin by monoclonal antibody increases bone formation, bone mass, and bone strength in aged male rats. J Bone Miner Res. 2010; 25:2647–56. [PubMed: 20641040]
11. Li X, Ominsky MS, Warmington KS, Morony S, Gong J, Cao J, Gao Y, Shalhoub V, Tipton B, Haldankar R, Chen Q, Winters A, Boone T, Geng Z, Niu QT, Ke HZ, Kostenuik PJ, Simonet WS, Lacey DL, Paszty C. Sclerostin antibody treatment increases bone formation, bone mass, and bone strength in a rat model of postmenopausal osteoporosis. J Bone Miner Res. 2009; 24:578–88. [PubMed: 19049336]
12. Ominsky MS, Vlasseros F, Jolette J, Smith SY, Stouch B, Doellgast G, Gong J, Gao Y, Cao J, Graham K, Tipton B, Cai J, Deshpande R, Zhou L, Hale MD, Lightwood DJ, Henry AJ, Popplewell AG, Moore AR, Robinson MK, Lacey DL, Simonet WS, Paszty C. Two doses of sclerostin antibody in cynomolgus monkeys increases bone formation, bone mineral density, and bone strength. J Bone Miner Res. 2010; 25:948–59. [PubMed: 20200929]
13. Ke HZ, Richards WG, Li X, Ominsky MS. Sclerostin and Dickkopf-1 as therapeutic targets in bone diseases. Endocr Rev. 2012; 33:747–83. [PubMed: 22723594]
14. Tian X, Jee WS, Li X, Paszty C, Ke HZ. Sclerostin antibody increases bone mass by stimulating bone formation and inhibiting bone resorption in a hindlimb-immobilization rat model. Bone. 2011; 48:197–201. [PubMed: 20850580]
15. Shahnazari M, Wronski T, Chu V, Williams A, Leeper A, Stolina M, Ke HZ, Halloran B. Early response of bone marrow osteoprogenitors to skeletal unloading and sclerostin antibody. Calcif Tissue Int. Jul; 2012 91(1):50–8. [PubMed: 22644321]

16. Macias BR, Swift JM, Nilsson MI, Hogan HA, Bouse SD, Bloomfield SA. Simulated resistance training, but not alendronate, increases cortical bone formation and suppresses sclerostin during disuse. J Appl Physiol. 2012; 112:918–25. [PubMed: 22174402]

17. Morey-Holton ER, Globus RK. Hindlimb unloading rodent model: technical aspects. J Appl Physiol. 2002; 92:1367–77. [PubMed: 11895999]

18. Devlin MJ, Cloutier AM, Thomas NA, Panus DA, Lotinun S, Pinz I, Baron R, Rosen CJ, Bouxsein ML. Caloric restriction leads to high marrow adiposity and low bone mass in growing mice. J Bone Miner Res. 2010; 25:2078–88. [PubMed: 20229598]

19. Parfitt AM. Bone histomorphometry: standardization of nomenclature, symbols and units (summary of proposed system). Bone. 1988; 9:67–9. [PubMed: 3377921]

20. Brodt MD, Ellis CB, Silva MJ. Growing C57Bl/6 mice increase whole bone mechanical properties by increasing geometric and material properties. J Bone Miner Res. 1999; 14:2159–66. [PubMed: 10620076]

21. Bouxsein ML, Boyd SK, Christiansen BA, Guldberg RE, Jepsen KJ, Muller R. Guidelines for assessment of bone microstructure in rodents using micro-computed tomography. J Bone Miner Res. 2010; 25:1468–86. [PubMed: 20533309]

22. Van Rietbergen B, Huiskes R, Eckstein F, Ruegsegger P. Trabecular bone tissue strains in the healthy and osteoporotic human femur. J Bone Miner Res. 2003; 18:1781–8. [PubMed: 14584888]

23. Robling AG, Warden S, Paszty C, Turner C. Sclerostin antibody protects the skeleton from disuse-induced bone loss. Oral Presentation 1039. J Bone Miner Res [Internet]. 2010; 25(Suppl 1):S13. [cited 2012 Nov 2]. Available from: http://onlinelibrary.wiley.com/doi/10.1002/jbmr.5650251301/pdf.

24. Stolina M, Dwyer D, Niu Q-T, Li X, Warmington K, Han CY, Salimi-Moosavi H, Simotet S, Kostenuik P, Ke HZ. Treatment with a sclerostin antibody increased osteoblast derived markers of bone formation and decreased osteoclast-related markers of bone resorption in ovariectomized rats. Oral Presentation SU0424. J Bone Miner Res [Internet]. 2010; 25(Suppl 1):S346. [cited 2012 Nov 2]. Available from: http://onlinelibrary.wiley.com/doi/10.1002/jbmr.5650251304/pdf.

25. Tu X, Rhee Y, Condon KW, Bivi N, Allen MR, Dwyer D, Stolina M, Turner CH, Robling AG, Plotkin LI, Bellido T. Sost downregulation and local Wnt signaling are required for the osteogenic response to mechanical loading. Bone. 2012; 50:209–17. [PubMed: 22075208]

26. Nakashima T, Hayashi M, Fukunaga T, Kurata K, Oh-Hora M, Feng JQ, Bonewald LF, Kodama T, Wutz A, Wagner EF, Penninger JM, Takayanagi H. Evidence for osteocyte regulation of bone homeostasis through RANKL expression. Nat Med. 2011; 17:1231–4. [PubMed: 21909105]

27. Ahdjoudj S, Lasmoles F, Holy X, Zerath E, Marie PJ. Transforming growth factor beta2 inhibits adipocyte differentiation induced by skeletal unloading in rat bone marrow stroma. J Bone Miner Res. 2002; 17:668–77. [PubMed: 11918224]

28. Takada I, Kouzmenko AP, Kato S. Wnt and PPARgamma signaling in osteoblastogenesis and adipogenesis. Nat Rev Rheumatol. 2009; 5:442–7. [PubMed: 19581903]

29. Ross SE, Hemati N, Longo KA, Bennett CN, Lucas PC, Erickson RL, MacDougald OA. Inhibition of adipogenesis by Wnt signaling. Science. 2000; 289:950–3. [PubMed: 10937998]

30. Qiu W, Andersen TE, Bollerslev J, Mandrup S, Abdallah BM, Kassem M. Patients with high bone mass phenotype exhibit enhanced osteoblast differentiation and inhibition of adipogenesis of human mesenchymal stem cells. J Bone Miner Res. 2007; 22:1720–31. [PubMed: 17680723]

31. Cristancho AG, Lazar MA. Forming functional fat: a growing understanding of adipocyte differentiation. Nat Rev Mol Cell Biol. 2011; 12:722–34. [PubMed: 21952300]

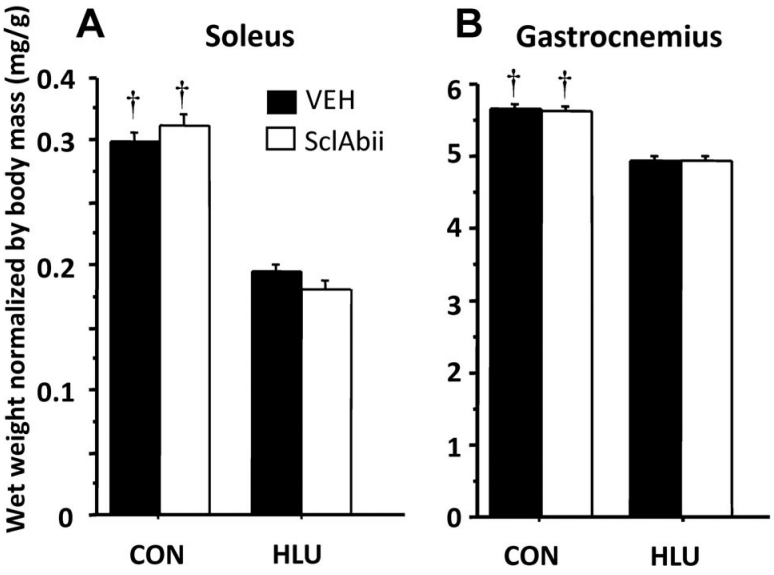

Fig. 1.

Effects of unloading and sclerostin antibody treatment on normalized wet weight of (*A*) soleus and (*B*) gastrocnemius muscles. †$p < 0.01$ for CON versus HLU within treatment group. Error bars represent 1 SEM.

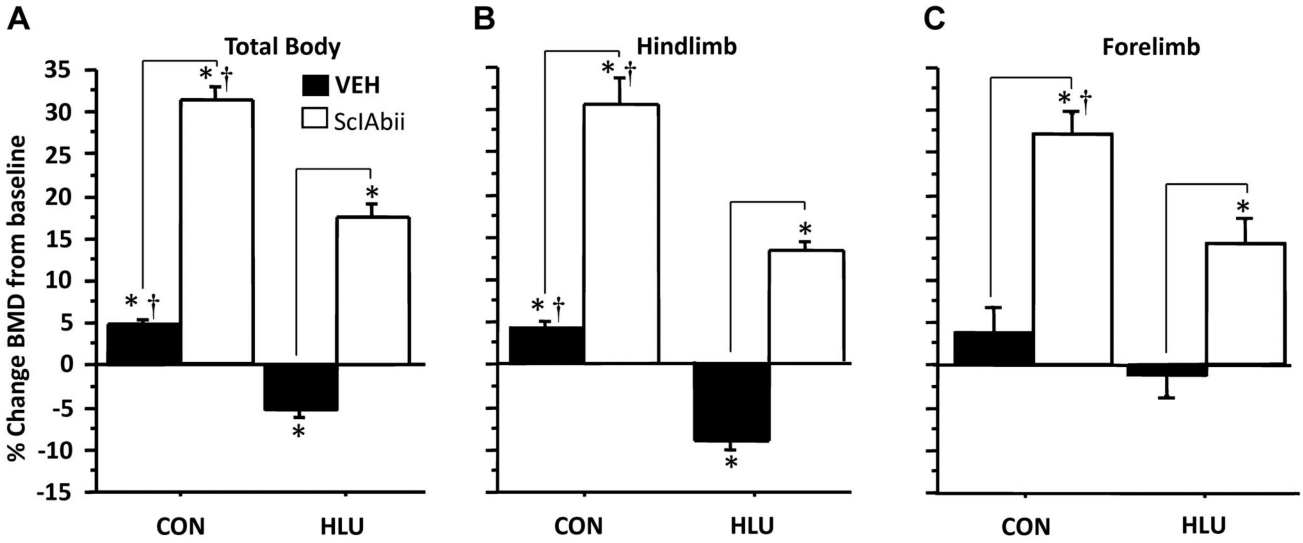

Fig. 2.

Effect of unloading and sclerostin antibody treatment on (*A*) total body BMD, (*B*) hindlimb BMD, and (*C*) forelimb BMD. *Significantly different from baseline ($p < 0.001$). Horizontal bars denote significant differences ($p < 0.01$) between VEH and SclAbII within loading groups; †$p < 0.05$ for CON versus HLU within a treatment group. Error bars represent 1 SEM. (One CON-SclAbII and three CON-VEH and animals were excluded from forelimb BMD measurements due to poor positioning on either baseline or follow-up scan.)

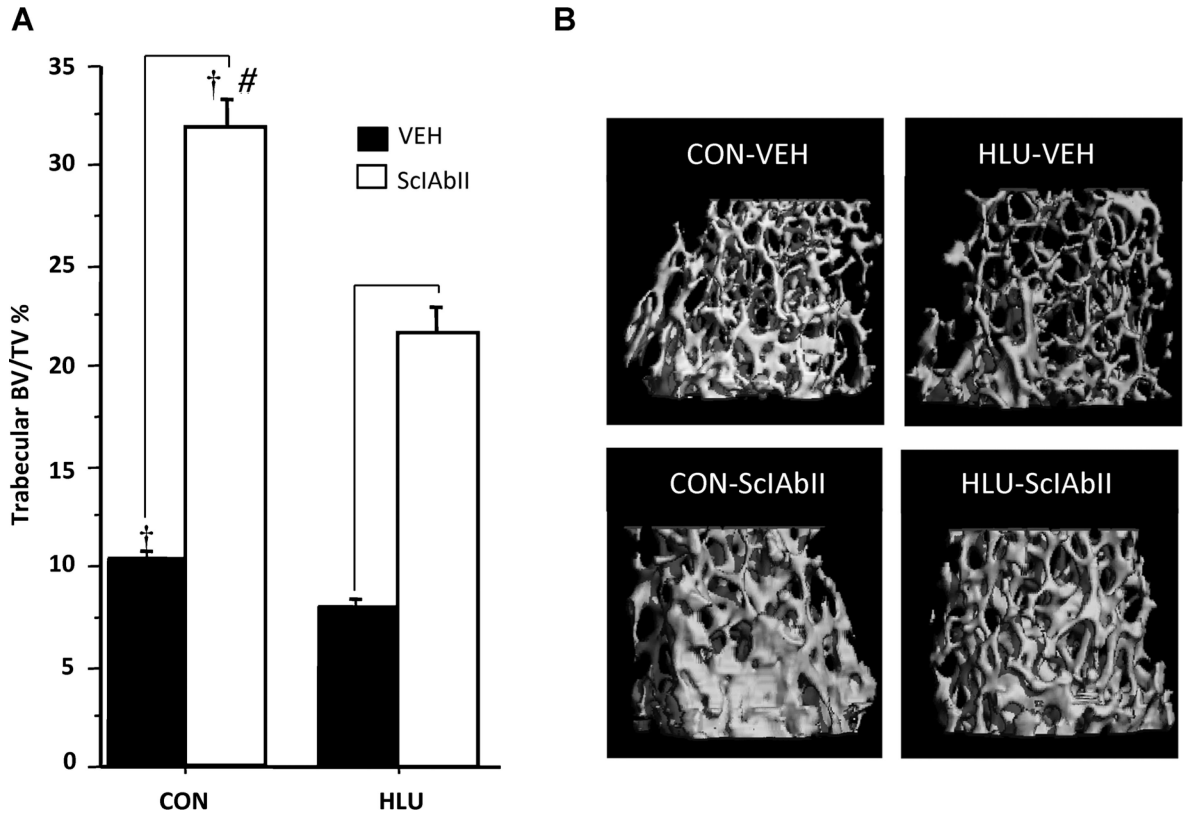

Fig. 3.

Effect of unloading and sclerostin antibody treatment at the distal femur. (*A*) trabecular BV/TV (%); (*B*) 3D rendering of μCT image from representative animals from each group. Horizontal bars designate significant differences between VEH and SclAbII within loading group ($p < 0.001$); †$p < 0.01$ for CON versus HLU within a treatment group; and #significantly greater effect of SclAbII in CON versus HLU. Error bars represent 1 SEM.

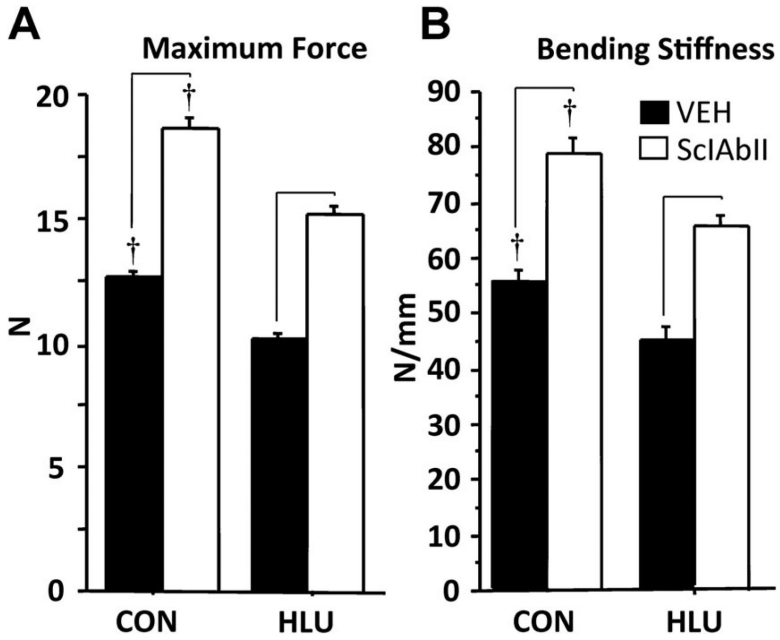

Fig. 4.

Effect of unloading and sclerostin treatment on femoral strength as assessed by three-point bending, (*A*) maximum force, and (*B*) bending stiffness. Horizontal bars designate significant differences between VEH and SclAbII within loading group ($p < 0.01$); †$p < 0.01$ CON versus HLU within a treatment group.

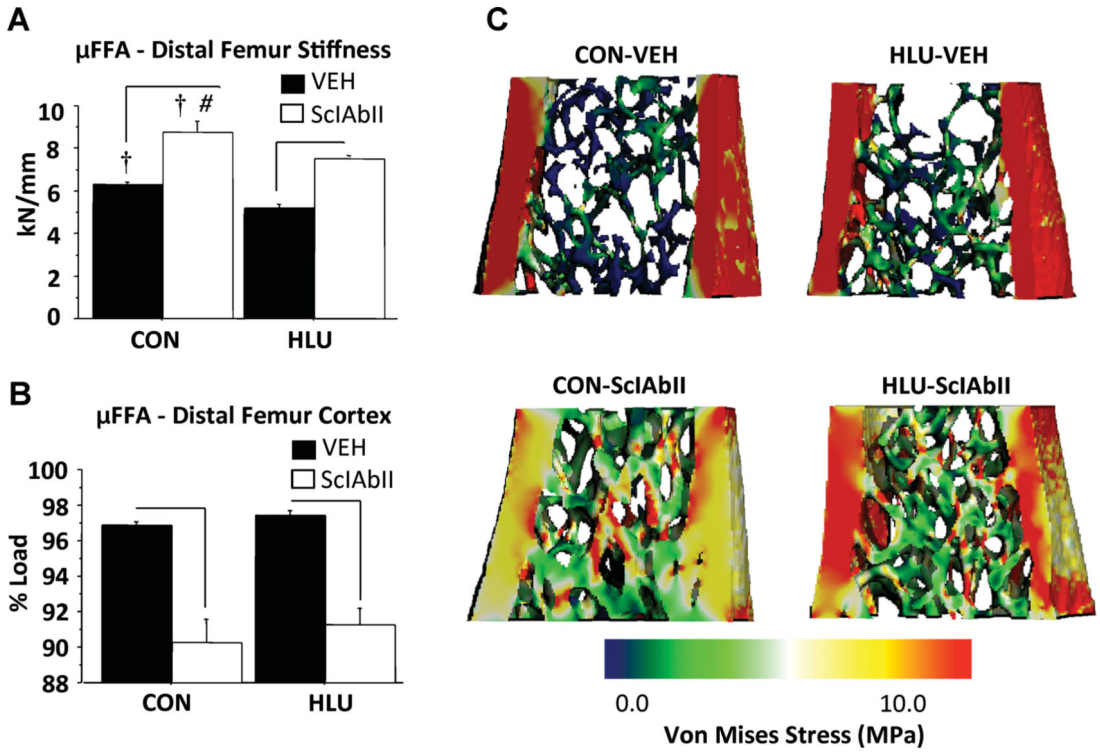

Fig. 5.

Effect of unloading and sclerostin antibody treatment on bone strength, as assessed by micro–finite element analysis (μFEA) of the distal femur: (*A*) stiffness, (*B*) % cortical load, (*C*) representative μFEA Von Mises Stress color map images. Horizontal bars designate significant differences between VEH and SclAbII within loading group ($p < 0.05$); †$p < 0.01$ for CON versus HLU within a treatment group; #significantly greater effect of SclAbII in CON versus HLU ($p < 0.02$); Error bars represent 1 SEM.

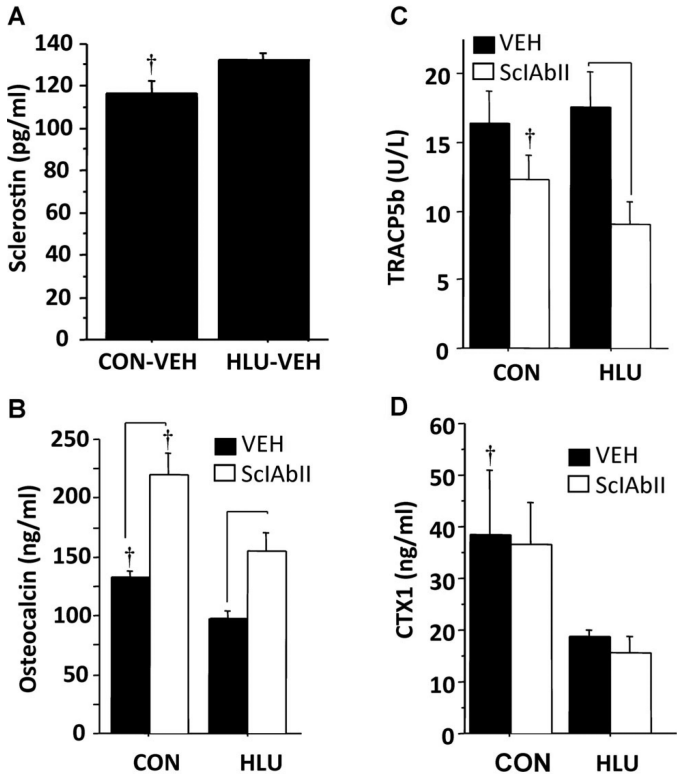

Fig. 6.

Effect of unloading and sclerostin antibody treatment on serum sclerostin and markers of bone turnover. (*A*) Sclerostin (vehicle groups only); (*B*) Osteocalcin; (*C*) TRACP5b, and (*D*) CTX1. Horizontal bars designate significant differences between VEH and SclAbII within loading group ($p < 0.05$). †$p < 0.01$ CON versus HLU within a treatment group. Error bars represent 1 SEM.

Table 1

Effect of HLU and SclAb-II Treatment on Femoral Trabecular and Cortical Bone Microarchitecture, Assessed by μCT

	Controls		HLU		ANOVA results		
Site	**Vehicle**	**SclAbII**	**Vehicle**	**SclAbII**	***p*load**	***p*treatment**	***p*interaction**
Distal trabecular							
BV/TV (%)	10.3 ± 0.4^{b}	$32.0 \pm 1.5^{a,b}$	8.0 ± 0.3	21.7 ± 1.2^{a}	<0.0001	<0.0001	<0.0001
Tb.N (mm^{-1})	3.86 ± 0.04^{b}	$4.32 \pm 0.05^{a,b}$	3.72 ± 0.05	4.05 ± 0.05^{a}	0.0006	<0.0001	0.1
Tb.Th (mm)	0.054 ± 0.001^{b}	$0.097 \pm 0.002^{a,b}$	0.048 ± 0.001	0.075 ± 0.003^{a}	<0.0001	<0.0001	<0.0001
Tb.Sp (mm)	0.252 ± 0.003^{b}	$0.198 \pm 0.003^{a,b}$	0.261 ± 0.003	0.217 ± 0.005^{a}	0.008	<0.0001	0.2
ConnD (mm^{-3})	74 ± 3^{b}	107 ± 3^{a}	55 ± 5	108 ± 3^{a}	0.3	<0.0001	0.06
SMI	2.99 ± 0.06	$1.4 \pm 0.12^{a,b}$	3.05 ± 0.05	1.98 ± 0.08^{a}	0.01	<0.0001	0.002
Distal cortical							
Tt.CSA (mm^2)	2.49 ± 0.03	$2.68 \pm 0.05^{a,b}$	2.48 ± 0.05	2.54 ± 0.05	0.3	0.008	0.9
Ct.BA (mm^2)	0.71 ± 0.01^{b}	$0.96 \pm 0.01^{a,b}$	0.57 ± 0.01	0.80 ± 0.02^{a}	<0.0001	<0.0001	0.7
Ct.BA/TA (%)	28.5 ± 0.4^{b}	$35.5 \pm 0.7^{a,b}$	22.8 ± 0.4	31.5 ± 0.2^{a}	<0.0001	<0.0001	0.06
Ct.Por (%)	5.9 ± 0.2^{b}	5.3 ± 0.2	7.9 ± 0.4	5.3 ± 0.4^{a}	0.0006	<0.0001	0.003
Ct.Th (mm)	0.12 ± 0.002^{b}	$0.15 \pm 0.002^{a,b}$	0.10 ± 0.001	0.13 ± 0.001^{a}	<0.0001	<0.0001	0.08
pMOI (mm^4)	0.50 ± 0.01^{b}	$0.71 \pm 0.02^{a,b}$	0.39 ± 0.01	0.57 ± 0.02^{a}	<0.0001	<0.0001	0.3
Midshaft cortical							
Tt.CSA (mm^2)	1.56 ± 0.018	$1.69 \pm 0.024^{a,b}$	1.54 ± 0.030	1.58 ± 0.026	0.03	0.001	0.05
Ct.BA (mm^2)	0.66 ± 0.010^{b}	$0.86 \pm 0.015^{a,b}$	0.55 ± 0.010	0.70 ± 0.012^{a}	<0.0001	<0.0001	0.02
Ct.MA (mm^2)	0.90 ± 0.014^{b}	0.83 ± 0.013^{a}	0.99 ± 0.023	0.88 ± 0.016^{a}	0.0004	<0.0001	0.2
Ct.BA/TA (%)	42.1 ± 0.5^{b}	$50.8 \pm 0.4^{a,b}$	35.8 ± 0.5	44.2 ± 0.3^{a}	<0.0001	<0.0001	0.04
Ct.Th (mm)	0.16 ± 0.002^{b}	$0.21 \pm 0.003^{a,b}$	0.13 ± 0.002	0.17 ± 0.002^{a}	<0.0001	<0.0001	0.03
TMD ($mgHA/cm^3$)	1148 ± 5	1161 ± 8	1135 ± 4	1147 ± 7	0.09	0.1	0.7
pMOI (mm^4)	0.28 ± 0.01^{b}	$0.37 \pm 0.01^{a,b}$	0.24 ± 0.01	0.29 ± 0.01^{a}	<0.0001	<0.0001	0.04

Values are mean ± SEM. BV/TV = bone volume fraction; CON = control; ConnD = connectivity density; Ct.BA = cortical bone area; Ct.BA/TA = cortical bone area fraction; Ct.MA = medullary area; Ct.Por = cortical porosity; Ct.Th = cortical thickness; HLU = hindlimb unloaded; pMOI = polar moment of inertia; SclAbII = sclerostin antibody; SMI = structure model index; Tb.N = trabecular number; Tb.Th = trabecular thickness; Tb.Sp = trabecular separation; TMD = tissue mineral density; Tt.CSA = total cross-sectional area; VEH = vehicle.

^{a} $p < 0.05$ SclAbII versus VEH within loading condition.

^{b} $p < 0.05$ CON versus HLU within treatment condition.

Table 2

Effect of HLU and SclAbll Treatment on Bone Microarchitecture at the Humerus

	Controls		HLU		ANOVA results		
	Vehicle	SclAbll	Vehicle	SclAbll	p_{load}	$p_{treatment}$	$p_{interaction}$
Proximal trabecular							
BV/TV (%)	9.2 ± 0.4	23.0 ± 1.3^{a,b}	8.5 ± 0.4	18.0 ± 1.0^{a}	0.004	0.0001	0.01
Tb.N (mm^{-1})	3.85 ± 0.07	4.55 ± 0.10^{a}	3.99 ± 0.07	4.30 ± 0.11^{a}	0.7	<0.0001	0.03
Tb.Th (mm)	0.049 ± 0.001	0.076 ± 0.001^{a,b}	0.047 ± 0.001	0.066 ± 0.001^{a}	<0.0001	<0.0001	0.008
Tb.Sp (mm)	0.26 ± 0.005	0.20 ± 0.006^{a}	0.25 ± 0.005	0.22 ± 0.007^{a}	1	<0.0001	0.04
ConnD (mm^{-3})	41 ± 4	87 ± 4^{a}	37 ± 5	83 ± 7^{a}	0.5	<0.0001	1
SMI	2.8 ± 0.05	2.0 ± 0.1^{a,b}	3.0 ± 0.06	2.2 ± 0.08^{a}	0.009	<0.0001	0.2
Midshaft cortical							
Tt.CSA (mm^2)	0.73 ± 0.01	0.80 ± 0.01^{a,b}	0.71 ± 0.01	0.75 ± 0.01^{a}	0.03	0.0001	0.2
Ct.BA (mm^2)	0.41 ± 0.006^{b}	0.54 ± 0.005^{a,b}	0.37 ± 0.009	0.48 ± 0.007^{a}	<0.0001	<0.0001	0.2
Ct.MA(mm^2)	0.32 ± 0.006^{b}	0.26 ± 0.006^{a}	0.35 ± 0.006	0.27 ± 0.006^{a}	0.009	<0.0001	0.3
Ct.BA/TA (%)	56.3 ± 0.3^{b}	67.7 ± 0.5^{a,b}	51.5 ± 0.5	64.0 ± 0.3^{a}	<0.0001	<0.0001	0.2
Ct.Por (%)	0.24 ± 0.02	0.20 ± 0.02	0.21 ± 0.005	0.20 ± 0.01	0.3	0.1	0.6
Ct.Th (mm)	0.16 ± 0.001^{b}	0.21 ± 0.002^{a,b}	0.14 ± 0.002	0.19 ± 0.001^{a}	<0.0001	<0.0001	0.2
TMD ($mgHA/cm^3$)	1174 ± 6	1167 ± 6	1153 ± 9	1171 ± 8	0.18	0.6	0.1
pMOI (mm^4)	0.072 ± 0.002^{b}	0.093 ± 0.002^{a,b}	0.065 ± 0.003	0.081 ± 0.003^{a}	0.0008	<0.0001	0.3

Values are mean ± SEM. BV/TV = bone volume fraction; CON = control; ConnD = connectivity density; Ct.BA = cortical bone area; Ct.BA/TA = cortical bone area fraction; Ct.MA = medullary area; Ct.Por = cortical porosity; Ct.Th = cortical thickness; HLU = hindlimb unloaded; pMOI = polar moment of inertia; SclAbll = sclerostin antibody; SMI = structure model index; Tb.N = trabecular number; Tb.Sp = trabecular separation; Tb.Th = trabecular thickness; TMD = tissue mineral density; Tt.CSA = total cross-sectional area; VEH = vehicle.

^{a} $p < 0.05$ SclAbll versus VEH within loading condition.

^{b} $p < 0.05$ HLU versus CON within treatment condition.

Table 3

Effect of Unloading and SclAbll Treatment on Static and Dynamic Quantitative Histomorphometry of the Distal Femur

	Controls		HLU	
	Vehicle	**SclAbll**	**Vehicle**	**SclAbll**
Static indices[a]				
N.Ob/BS (#/mm^2)	24 ± 4	23 ± 2	26 ± 4	32 ± 2
N.Oc/BS (#/mm^2)	3.9 ± 1.1	4.4 ± 1.0	6.5 ± 1.3	5.1 ± 1.3
N.Ot/BA (#/mm^2)	740 ± 44	591 ± 34	653 ± 93	647 ± 38
N.Ad/MA (#/mm^2)	16 ± 4**	17 ± 4**	34 ± 7	35 ± 6
Ad.Diam (μm)	44.0 ± 2.5***	36.0 ± 1.1**	51 ± 4	50.5 ± 2.4
OS/BS (%)	24.0 ± 2.0	25.7 ± 2.0	25.2 ± 5.0	33.7 ± 2.0
ES/BS (%)	6.3 ± 1.5	6.3 ± 0.7	8.7 ± 1.9	10.1 ± 2.4
Dynamic indices[b]				
MS/BS (%)	13.6 ± 3.3	24.9 ± 2.2*	11.6 ± 5.5	21.1 ± 5.0*
MAR (|μm/d)	1.2 ± 0.2**	1.6 ± 0.2*	0.5 ± 0.2	2.0 ± 1.1*
BFR/BS (|μm^3/|μm^2/d)	0.2 ± 0.1	0.4 ± 0.1*	0.09 ± 0.1	0.9 ± 0.6*

Values are mean ± SEM. Ad.Diam = adipocyte diameter; BFR/BS = bone formation rate per bone surface; CON = controls; ES/BS = eroded surface per bone surface; HLU = hindlimb unloaded; MAR = mineral apposition rate; MS/BS = mineralizing surface; N.Ad/MA = adipocyte number per marrow area; N.Ob/ BS = osteoblast number per bone surface; N.Oc/BS = osteoclast number per bone surface; N.Ot/BA = osteocyte number per bone area; OS/BS = osteoid osteoid surface per bone surface; SclAbll = sclerostin antibody; VEH = vehicle.

[a] Sample size for static indices: n = 6/group.

[b] Sample size for dynamic indices: CON-VEH, *n* = 6; CON-SclAbll, *n* = 5; HLU-VEH, *n* = 3; HLU-SclAbll, *n* = 3.

* $p < 0.05$ SclAbll versus VEH treatment within the CON or HLU groups.

** $p < 0.05$ HLU versus CON within the SclAbll and VEH treatment groups.

*** $p = 0.08$ HLU versus CON within VEH-treated group.